Wetting of ^{3}He-^{4}He mixtures on cesium and other alkali metals

M. S. Pettersen
Department of Physics and Astronomy, Otterbein College, Westerville, Ohio 43081

W. F. Saam
Department of Physics, The Ohio State University, Columbus, Ohio 43210
(Received 12 January 1995)

From available information concerning the wetting behavior of pure ^{3}He and pure ^{4}He on alkali-metal substrates, as well as the known properties of bulk ^{3}He-^{4}He mixtures, we derive the complete wetting phase diagrams for such mixtures, showing prewetting, isotopic separation, and lambda transitions for the film phases. Mixture films form a rich system because the chemical potentials of ^{3}He and ^{4}He can be varied independently. We predict phenomena such as a triple-point-induced dewetting transition, and the absence of a superfluid-film-wetting Cs, Rb, and K walls under concentrated ^{3}He solutions. Experimental methods for testing the predictions are suggested.

I. INTRODUCTION

The physics of wetting transitions has been transformed with the recent prediction[1,2] and subsequent experimental observation of wetting and prewetting transitions in ^{4}He adsorbed on cesium[3–7] and H_2 adsorbed on rubidium.[8] It was soon realized[9] that the addition of a small amount of ^{3}He, which behaves as a surfactant, could augment wetting of ^{4}He on Cs, indeed producing reentrant wetting phenomena recently observed by Ketola and Hallock.[10] In this work we explore the full range of concentrations in ^{3}He-^{4}He mixtures on Cs and other alkali metals.

Our exposition begins in Sec. II with the construction of the bulk phase diagram for ^{3}He-^{4}He mixtures in μ_3-μ_4-T space. This construction, shown in Figs. 1 and 2, sets the stage for our discussion of wetting phenomena.

In Sec. III we turn our attention to the case of helium mixtures adsorbed on Cs substrates. The resultant phase diagrams, shown in Figs. 3–7, predict fascinating new phenomena, including triple-point dewetting, which has yet to be observed experimentally.

Section IV is devoted to the construction of the phase diagrams for helium mixture adsorption on alkali-metal substrates other than cesium. The case of sodium is considered first as an example where, unlike for cesium, there is no region of nonwetting and triple-point dewetting is absent. We note that the phase diagram for Na substrates may well be representative of most strongly binding substrates once solid helium layers are accounted for. Rubidium and potassium may be in a class intermediate between sodium and cesium, with both ^{4}He and ^{3}He wetting and prewetting at $T = 0$ as well as ^{3}He triple-point dewetting.

Further discussion and conclusions appear in Sec. V. Experimental tests of our results are proposed, and it is pointed out that our prediction that ^{4}He films will not wet Cs, Rb, or K substrates under bulk concentrated ^{3}He could possibly allow Bose condensation of ^{4}He quasiparticles in supersaturated solutions of ^{4}He in ^{3}He.

II. CONSTRUCTION OF THE BULK PHASE DIAGRAM

It is illuminating to present the film phase diagram against the background of the bulk phase diagram. The complete phase diagram of liquid helium mixtures in μ_3-μ_4-T space is shown in Fig. 1. The main features of this diagram are the liquid-vapor coexistence or saturated vapor pressure (SVP) sheet *atbcd*, the isotopic phase separation sheet t_3eft, and the λ line lt_3. The λ

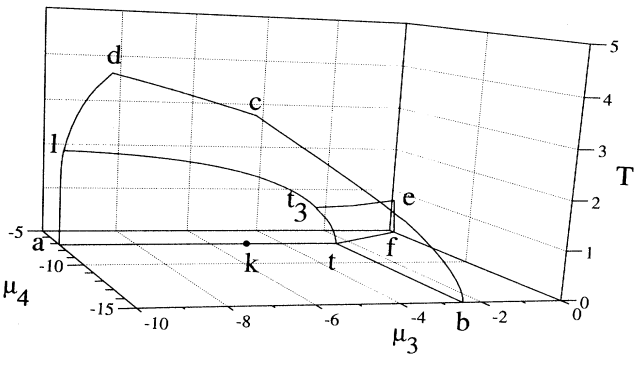

FIG. 1. The complete phase diagram of bulk ^{3}He-^{4}He mixtures in μ_3-μ_4-T space. The sheet *atbcd* is the liquid-vapor coexistence sheet with critical line *cd*; the sheet $tfet_3$ is the isotopic separation sheet with tricritical line t_3e. The curve lt_3e shows two edges of the λ sheet. Point k is a transition of the ^{4}He surface at which the Andreev states start to become occupied by ^{3}He. μ_3, μ_4, and T are in K.

line is the intersection of the superfluid transition sheet (on the liquid side of the SVP sheet but not shown) and the SVP sheet. The line t_3t is a triple line, ending in the tricritical point t_3. Note that the SVP sheet has a crease at the triple line. There is, in addition, as discussed in more detail below, a line of second-order transitions (see Fig. 2) in the $T = 0$ plane representing the limit of solubility of ^{3}He in ^{4}He.

A. $T = 0$

In order to understand the construction of the bulk phase diagram, it is simplest to consider the zero-temperature case first. The corresponding phase diagram is shown in Fig. 2.

1. *Liquid-gas coexistence: Condensation at 0 K*

Here we consider the curve forming the edge of the liquid-vapor coexistence sheet at 0 K. The slope of this line is determined by a Clausius-Clapeyron equation

$$\left.\frac{d\mu_4}{d\mu_3}\right|_{\text{coex}} = -\frac{\Delta n_3}{\Delta n_4}, \tag{1}$$

where Δn_3 and Δn_4 are the discontinuities in the ^{3}He and ^{4}He number densities across the line. Since the vapor phase has zero density at $T = 0$, $\Delta n_3/\Delta n_4 = X_3/X_4$, where X_i refers to the concentration of the ith isotope in the liquid. At 0 K, ^{4}He is insoluble in ^{3}He, and so the condensation line, tb of Fig. 2, for ^{3}He lies at $\mu_3 = -L_3$, where the latent heat of ^{3}He is L_3=2.473 K.[11] Since ^{3}He has a binding energy in ^{4}He of E_3=2.785 K,[12] for chemical potentials $\mu_3 < -E_3$, ^{3}He does not dissolve in ^{4}He and the condensation curve, as shown in Fig. 2, lies at $\mu_4 = -L_4$, where the latent heat of ^{4}He is $L_4 = 7.16$ K. For weak solutions of ^{3}He in ^{4}He, the ^{3}He acts like a Fermi gas of quasiparticles of mass $m_3^* = 2.272m_3$,[13,14] where m_3 is the bare ^{3}He mass. The number density of ^{3}He is then

$$n_3 = \frac{1}{3\pi^2\hbar^3}[2m_3^*(\mu_3 + E_3)]^{3/2}, \tag{2}$$

which can be integrated with the assumption that the number density n_4 of ^{4}He remains approximately constant to give

$$\mu_4 + L_4 = -\frac{2(2m_3^*)^{3/2}}{15\pi^2\hbar^3 n_4}(\mu_3 + E_3)^{5/2} \equiv -\pi_3/n_4 \tag{3}$$

as the equation for the condensation curve for the solution. [The right-hand side of Eq. (3) defines the osmotic pressure π_3.] This curve is denoted as st in Fig. 2. In practice, we have adjusted the coefficient of $(\mu_3 + E_3)$ slightly to match the data of Radebaugh.[15] The zero-temperature triple point t is just the intersection of the curve of Eq. (3) with the line $\mu_3 = -L_3$.

2. *Liquid mixture coexistence at $T = 0$*

To find the edge (the line tf of Fig. 2) of the isotopic separation sheet at 0 K, we use the Clausius-Clapeyron equation to find

$$\left.\frac{d\mu_4}{d\mu_3}\right|_{\text{coex}} = -\frac{\Delta n_3}{\Delta n_4} = \frac{v_d/v_3 - X_3}{X_4} = 0.75, \tag{4}$$

where the specific volumes of the dilute phase and pure ^{3}He are $v_d = 28.1$ cm^3/mol (Ref. 16) and $v_3 = 36.818$ cm^3/mol, respectively.[17]

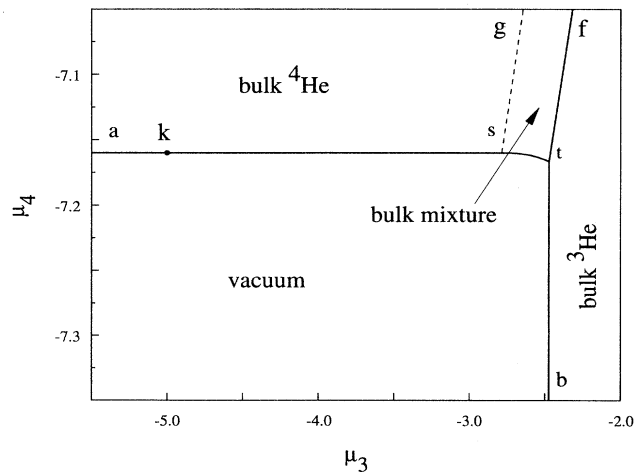

FIG. 2. The phase diagram of ^{3}He-^{4}He mixtures at $T = 0$. Curve atb is the liquid-vapor coexistence transition; tf is the isotopic separation transition; sg is a second-order transition at which ^{3}He becomes soluble in ^{4}He; k is the same as in Fig. 1. μ_3 and μ_4 are in K.

3. *Solubility curve*

The limiting point of solubility of ^{3}He in ^{4}He varies with pressure as[18] $dE_3/dp = -(1 + \alpha_3)n_4$, leading to a second-order transition line, shown as the dashed line sg in Fig. 2, in the $T = 0$ plane with a slope

$$d\mu_3/d\mu_4 = -(dE_3/dp)(\partial p/\partial\mu_4) = 1 + \alpha_3, \tag{5}$$

where α_3=0.286 at SVP.[19] This transition occurs only at T=0, since at nonzero temperatures there is a nonzero concentration of ^{3}He at all μ_3.

4. *Surface solubility of ^{3}He*

There exists a bound state[20] of the ^{3}He atom at the surface of bulk ^{4}He with a binding energy of E_s=2.22 K with respect to E_3, the binding energy to the bulk.[21] Thus below $\mu_3 = -(E_s + E_3) = -5$ K, the surface of bulk ^{4}He is bare of ^{3}He; above, ^{3}He atoms are bound to the surface (though insoluble in the bulk for $\mu_3 < -E_3$).

Like the previous transition, this transition, marked k in Figs. 1 and 2, occurs only at 0 K, and is second order.

B. Extension to $T > 0$

The extension of the phase diagram of Fig. 2 to $T > 0$ consists of extending the solid lines as sheets which eventually terminate in critical lines and in adding the λ transition sheet.

1. *Liquid-gas coexistence: Critical line*

The liquid-vapor coexistence sheet, which terminates at $T = 0$ in the curve $astb$ of Fig. 2 ends in the critical line dc of Fig. 1. To determine this critical line, we use the phenomenological interpolation formula of Leung and Griffiths.[22] In terms of the parameter ζ, which goes from 0 for pure ^{3}He to 1 for pure ^{4}He, the critical line is given by

$$T = \frac{1}{\frac{1}{T_{c3}} - \left(\frac{1}{T_{c3}} - \frac{1}{T_{c4}}\right)\zeta},$$

$$\mu_3 = T[b_1\zeta + b_2\zeta^2 + \ln(1-\zeta) - \ln C_3] + A_3,$$

$$\mu_4 = T[b_1\zeta + b_2\zeta^2 + \ln(\zeta) - \ln C_4] + A_4, \qquad (6)$$

with the critical temperature of ^{3}He T_{c3}=3.3105 K, the critical temperature of ^{4}He T_{c4}=5.1884 K, b_1=0.25, b_2=0.2568, $\ln C_3$=1.683, and $\ln C_4$=2.931. The constants A_3 and A_4 are left arbitrary by Leung and Griffiths, but may be determined if we know the chemical potentials at the critical points of pure ^{3}He and ^{4}He. The chemical potential at SVP, $\mu_4^0(T)$, is given from T=2 K to T_{c4} by Sychev *et al.*,[23] who give $\mu_4^0(T_{c4}) = -10.96$ K. To our knowledge, the analogous quantity for ^{3}He has not been calculated. We use the calculations of Radebaugh[15] for $\mu_3^0(T)$ up to T=1.5 K, and observe that its second derivative extrapolates nicely to the value $d^2\mu/dT^2 = -0.22$ $K^{-2}p_cv_c/k_B$ at the critical point given by Wallace and Meyer.[24] (In this formula, p_c=861 Torr and v_c=24.2 cm^3/g are the pressure and specific volume at T_c=3.31 K.[24]) The spline integration routine of the plotting package PSIPLOT (Ref. 25) then gives $\mu_3^0(T_{c3}) = -6.8$ K. In Table I, we present the complete curves of $\mu_3^0(T)$ and $\mu_4^0(T)$ at SVP for both pure isotopes, where the data below 1.5 K come from Ref. 15 for both ^{3}He and ^{4}He, and the data for ^{4}He above 2 K are from Ref. 23. For ^{4}He between 1.5 K and 2 K the data are interpolations using a fitted function $\mu_4^0(T) = -(L_4 + 0.001T^{7.4})$, with μ_4^0, L_4, and T in K. For ^{3}He above 1.5 K, they are the result of interpolation and the extrapolation described above. A good fit to the ^{3}He data is given by the function $\mu_3^0(T) = -(E_3 + 0.225T + 0.544T^2 - 0.0675T^3)$, with μ_3^0, E_3, and T in K. Finally, we find $A_3 = -1.24$ K and $A_4 = 1.62$ K.

TABLE I. The complete curves of $\mu_3^0(T)$ and $\mu_4^0(T)$ at SVP for both pure isotopes. Data below T = 1.5 K are from Ref. 15; data for ^{4}He above T = 2 K are from Ref. 23; other data are interpolation and extrapolation as described in the text.

T (K)	$\mu_3^0(T)$ (K)	T (K)	$\mu_4^0(T)$ (K)
0.00	-2.4730	0.00	-7.1600
0.10	-2.4867	0.80	-7.1602
0.20	-2.5229	1.00	-7.1610
0.30	-2.5754	1.20	-7.1638
0.40	-2.6400	1.40	-7.1718
0.50	-2.7142	1.60	-7.1916
0.60	-2.7964	1.80	-7.2356
0.80	-2.9810	2.00	-7.3250
1.00	-3.1888	2.20	-7.4811
1.20	-3.4170	2.40	-7.6429
1.40	-3.6644	2.80	-8.0083
1.60	-3.9565	3.20	-8.4213
1.80	-4.2574	3.60	-8.8753
2.00	-4.5734	4.00	-9.3683
2.20	-4.9014	4.40	-9.8974
2.40	-5.2382	4.80	-10.4607
2.60	-5.5807	5.20	-10.9600
2.80	-5.9257		
3.00	-6.2701		
3.20	-6.6107		
3.32	-6.8119		

2. *Triple line*

For the triple line tt_3 of Fig. 1 we use the data of Radebaugh[15] for the concentration X_3 in the ^{3}He-rich phase at phase separation up to T=0.6 K, together with the values X_3=0.67 and T=0.87 K at the tricritical point at SVP. The chemical potential μ_3 can be determined from X_3 and T from the Gibbs function $G = X_3\mu_3^0(T) + X_4\mu_4^0(T) - TS_m + G_E$, where $S_m = -k_B(X_3 \ln X_3 + X_4 \ln X_4)$ is the entropy of mixing, and G_E represents the deviation from the behavior of an ideal mixture. If the vapor pressure can be neglected, then $\mu_3 = (G + X_4\partial G/\partial X_3)$. Below 1.2 K, the excess Gibbs function agrees with the regular solution model, $G_E = k_BWX_3X_4$, if the parameter W is allowed to depend on T.[15,26] Then $\mu_3 = \mu_3^0(T) + WX_4^2 + T\ln X_3$. For 0.2K< T <0.6 K, Radebaugh's values of W are fitted by the function $W = 1.027 + 0.511T + 0.441T^2$, with W and T in K. At 0.87 K, we can use the value W=1.54 K.[26]

For μ_4 along the triple line, we use the formula for the osmotic pressure given by Van de Klundert *et al.*,[27] $\pi_3 = 16.9 + 640T^2$ torr (if T is in K) and compute $\mu_4(X_3, T) = \mu_4^0(T) - \pi_3/n_4$.

3. *Tricritical line*

The isotopic phase separation sheet $tfet_3$ of Fig. 1 ends in the tricritical line t_3e. del Cueto *et al.*[28] give values for

X_3 and T at the tricritical point as a function of pressure p. To determine μ_3 and μ_4 from these values, we observe that X_3 and T do not vary greatly along the tricritical line; then we can use

$$\left(\frac{\partial\mu_4}{\partial p}\right)_{X_3,T} = (1+\alpha_4)v_3(p,T) \tag{7}$$

and

$$\left(\frac{\partial\mu_3}{\partial p}\right)_{X_3,T} = (1+\alpha_3)v_4(p,T), \tag{8}$$

where α_4 has been measured by Laheurte,[29] $\alpha_3(p)$ by Watson *et al.*,[19] and values of the specific volumes of the pure isotopes v_3 and v_4 are taken from Wilks.[30] Numerical integration using PSIPLOT yields the tricritical line.

4. λ line

To complete the bulk phase diagram, we observe that the λ line, the curve lt_3 of Fig. 1 (λ transition at SVP) is well known in X_3-T (Ref. 31) space. To convert from X_3 and T to μ_3 and μ_4, we use the regular solution model of Sec. II A 2. Above 1.2 K, helium mixtures deviate slightly from regular solution behavior. However, a fit of the regular solution model with $W = 1.49 + 0.344(T - 0.6) - 0.379(T-0.6)^2$ fits all the data of de Bruyn Ouboter *et al.*[26] within 0.2 K over the range of data 0.9 K< T <1.7 K. The λ sheet extends from its termination lt_3 on the liquid-gas coexistence sheet back into the liquid region of the phase diagram. As this sheet does not interest us directly here, we do not display its location.

III. CONSTRUCTION OF THE FILM PHASE DIAGRAM FOR CESIUM SUBSTRATES

Again, it is instructive to consider the zero-temperature case first.

A. $T = 0$ film phase diagram for Cs substrates

Figure 3 shows the phase diagram of ^{4}He films on Cs. The diagram is that of the bulk with the prewetting curve WXY and the film isotopic separation curve XD added.

1. $T = 0$ prewetting curve

It follows from the appropriate Clausius-Clapeyron equation that the 0 K condensation line XY for the pure ^{3}He film is a vertical line at the chemical potential $\mu_3 = -2.70$ K deduced by Pricaupenko and Treiner.[32] The wetting transition W for the pure ^{4}He film is at $\mu_3 = -3.4$ K, as determined by us earlier.[9] To determine the shape of the prewetting curve near W we write Eq. (1), at $T = 0$, as

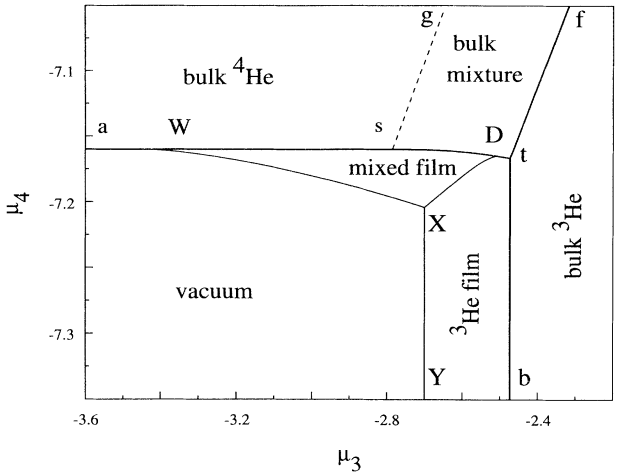

FIG. 3. The phase diagram of ^{3}He-^{4}He mixture films adsorbed on Cs at $T = 0$. Bulk phase transitions are reproduced from Fig. 2; WXY is a prewetting (thin-thick) transition in the film; XD is the isotopic separation transition in the film. W is a wetting transition, D a dewetting transition. μ_3 and μ_4 are in K.

$$\frac{d\mu_4}{d\mu_3} = -\frac{N_3}{N_4}, \tag{9}$$

where N_3 and N_4 are the ^{3}He and ^{4}He numbers in the film. Near W the film is very thick, and all the ^{3}He atoms are on the film's surface. The film's thickness z_4 is controlled by $\Delta\mu_4 = \mu_4 - \mu_4^0$ and found by minimizing the energy

$$\omega_{4f}(z_4) = \frac{\rho_4\Delta C_3^{4w}}{2z_4^2} - \rho_4\Delta\mu_4 z_4, \tag{10}$$

where

$$\Delta C_3^{4w} = C_3^{4w} - C_3^{44} \tag{11}$$

is the effective strength[33] of the van der Waals force, C_3^{4w} is the strength of the van der Waals force between a ^{4}He atom and the wall, and C_3^{44} is the analogous quantity for a ^{4}He atom and a ^{4}He "substrate." The minimization gives

$$z_4 = \left(\frac{\Delta C_3^{4w}}{-\Delta\mu_4}\right)^{1/3}, \tag{12}$$

and, as $N_4 = z_4\rho_4$, Eq. (9) becomes

$$\frac{d\mu_4}{d\mu_3} = -\frac{n_{3s}}{\rho_4}\left(\frac{-\Delta\mu_4}{\Delta C_3^{4w}}\right)^{1/3}, \tag{13}$$

where n_{3s} can be taken equal to the coverage (0.7 layers) at W. This integrates to

$$\Delta\mu_4 = -\left(\frac{2n_{3s}\Delta\mu_3}{3\rho_4(\Delta C_3^{4w})^{1/3}}\right)^{3/2} \quad (14)$$

$$= -\left(\frac{\Delta\mu_3}{5.93}\right)^{3/2}, \quad (15)$$

where $\Delta\mu_3$ is measured from W. We in fact use this result, extrapolated to its intersection with XY to estimate the location of the point X at $\mu_3 = -2.7$ K and $\mu_4 = -7.2$ K.

2. Dewetting transition

The isotopic phase separation curve runs from X to D. To determine the location of the point D, we first consider the state of the film at the triple point t. We let the surface tensions of the wall-dilute phase interface, the dilute phase-pure ^{3}He interface, the pure ^{3}He-vapor interface, and the wall-pure ^{3}He interface be σ_{wd}, σ_{d3}, σ_{3v}, and σ_{w3}, respectively. Both the pure ^{3}He film and the dilute ^{4}He film wet Cs at t, and the dilute film is wetted by a surface layer of ^{3}He.[21] Hence the surface excess free energies of the dilute film phase and the concentrated (pure ^{3}He at $T = 0$) film phase are, respectively, $\omega_{df} = \sigma_{wd} + \sigma_{d3} + \sigma_{3v}$ and $\omega_{cf} = \sigma_{w3} + \sigma_{3v}$.

Saam and Treiner[34] have calculated that

$$\sigma_{wd} + \sigma_{d3} - \sigma_{w3} = 0.013 \text{ K/Å}^2, \quad (16)$$

which implies that $\omega_{df} - \omega_{cf} = +0.013$ K/Å$^2 > 0$, from which it follows that the concentrated phase is the stable phase at the point t. (Note that the result[34] $\sigma_{wd} + \sigma_{d3} - \sigma_{w3} > 0$ implies that a layer of ^{4}He *does not* form at the interface between pure ^{3}He and cesium, raising the possibility of forming supersaturated solutions of ^{4}He in ^{3}He in cesium-coated vessels.) Since the pure ^{3}He film is wetting only along the bulk coexistence curve tb, it is nonwetting along the stretch of curve Dt, and so the point D is a triple-point-induced dewetting transition[35] from a wetting dilute film to a nonwet ^{3}He film.

We remark that triple-point dewetting is the case when each of two phases wets the wall individually, but near the triple point where both phases coexist with the vapor, a narrow interval of nonwetting behavior is introduced. This is to be distinguished from the case of triple-point wetting, where one of the phases wets and the other does not, and the triple point is the boundary between the two behaviors.[36]

To determine the location of the point D more precisely, we need a model of the surface excess free energy density of the two phases away from the bulk coexistence curve atb. For the concentrated film along the curve Dt, our model is

$$\omega_{cf} = \sigma_{3v} + \sigma_{w3} + \rho_3\Delta C_3^{3w}/2z_3^2 - z_3\rho_3\Delta\mu_3, \quad (17)$$

where z_3 is the thickness of the film, ρ_3 is the ^{3}He liquid density, and $\Delta\mu_3 = \mu_3 - \mu_3^0$ is the difference in chemical potential from the chemical potential of the bulk-saturated liquid (line tb). The thickness of the film is derived by minimizing the free energy with respect to z_3, whence

$$z_3 = \left(\frac{-\Delta C_3^{3w}}{\Delta\mu_3}\right)^{1/3}. \quad (18)$$

For the dilute film along the curve aD, the same analysis yields

$$\omega_{df} = \sigma_{3v} + \sigma_{d3} + \sigma_{wd} + \rho_3\Delta C_3^{3d}/2z_{c(df)}^2 - z_{c(df)}\rho_3\Delta\mu_3, \quad (19)$$

where $z_{c(df)}$, the thickness of the ^{3}He layer on top of the thick dilute film, is given by

$$z_{c(df)} = \left(\frac{-\Delta C_3^{3d}}{\Delta\mu_3}\right)^{1/3}. \quad (20)$$

In the above, ΔC_3^{3w} and ΔC_3^{3d} are defined in obvious analogy to ΔC_3^{4w} in Eq. (11). The point D is then determined by the condition that the concentrated film and the dilute film have equal surface excess free energy. The result is

$$\frac{3}{2}\rho_3\left[(\Delta C_3^{3w})^{1/3} - (\Delta C_3^{3d})^{1/3}\right](-\Delta\mu_3)^{2/3} = \sigma_{wd} + \sigma_{d3} - \sigma_{w3}, \quad (21)$$

whence $\Delta\mu_3 = -0.034$ K. (Here we use $\Delta C_3^{3d} \approx \Delta C_3^{34}$.) Note that this implies that the concentration of ^{3}He in the dilute solution at D is only 5.2%;[16] dilute solutions of concentration greater than this, though stable in the bulk, will not wet cesium at T=0 K.

3. Isotopic separation in the film

We next wish to consider the asymptotic form of the isotopic separation line XD for the film.

When the chemical potential departs from the bulk-saturated vapor pressure curve for the dilute solution, the thickness of the dilute layer of the film varies rapidly, while the thickness of the ^{3}He layer on top of the film varies relatively slowly. Therefore it suffices to take for the free energy of the dilute film

$$\omega_{df} = \text{const} + \rho_d\Delta C_3^{dw}/2z_{d(df)}^2 + z_{d(df)}\Delta\omega_d, \quad (22)$$

where $z_{d(df)}$ is the thickness of the dilute layer of the stratified dilute film, and ω_d is the bulk Landau free energy density. $\Delta\omega_d$ is the free energy cost of having a liquid phase in the region of the phase diagram where the vapor has lower free energy. The Landau free energy is the appropriate choice of free energy, since we wish to extrapolate the free energy of the dilute phase away from the saturated vapor pressure curve in the μ_3-μ_4 plane. At constant T,

$$d\omega_d = -\rho_d(X_{3d}d\mu_3 + X_{4d}d\mu_4),$$

where X_{id} is the concentration of the ith helium isotope

in the dilute layer. Close to the saturated vapor curve, we integrate this equation at constant X_{3d} to find

$$\Delta\omega_d = -\rho_d(X_{3d}\Delta\mu_3 + X_{4d}\Delta\mu_4), \tag{23}$$

where $\Delta\mu_3$ and $\Delta\mu_4$ represent the difference in chemical potentials between the actual state of the film (μ_3, μ_4) and a "reference" bulk liquid state $(\mu_3^{\rm ref}, \mu_4^{\rm ref})$ at the same concentration. To first order, because of the Clausius-Clapeyron equation governing the saturated vapor curve, $d\mu_4/d\mu_3|_{T,SVP} \approx -X_{3d}/X_{4d}$ (neglecting the density of the vapor), the right-hand side of Eq. (23) is actually invariant with respect to the choice of the bulk reference state: It can be any nearby bulk liquid state of any concentration at the saturated vapor pressure (the reference state must be the dilute phase, of course). We may then drop the requirement that $\Delta\mu_3$ and $\Delta\mu_4$ correspond to a path of constant X_{3d}.

For convenience, we define

$$\Delta\mu' = -\Delta\omega_d/\rho_d \approx X_{3d}\Delta\mu_3 + X_{4d}\Delta\mu_4. \tag{24}$$

Because of the Clausius-Clapeyron equation, $\Delta\mu'$ approximately measures the perpendicular distance from the saturated vapor pressure curve in the μ_3-μ_4 plane.

We can now derive the asymptotic form of XD near the point t from the Clausius-Clapeyron equation for the film, $d\mu_4/d\mu_3|_{T,\text{coexistence}} = (N_{3(df)} - N_{3(cf)})/(N_{4(cf)} - N_{4(df)})$, where the N_3's and N_4's are the total coverages of ^{3}He and ^{4}He in the two film phases, the dilute film and the concentrated film. We need to find these coverages to complete the analysis. Once again, the thickness of the concentrated film is slowly varying near the point D, and it consists of pure ^{3}He with a coverage $N_{3(cf)}$.

We next find the coverages for the stratified dilute film. The thickness of the dilute layer can be determined by minimizing Eq. (22). We therefore have

$$z_{d(df)} = \left(\frac{-\Delta C_3^{dw}}{\Delta\mu'}\right)^{1/3}. \tag{25}$$

For the dilute film the total coverages are

$$N_{3(df)} = N_{c(df)} + X_{3d}\rho_d z_{d(df)} \tag{26}$$

and

$$N_{4(df)} = X_{4d}\rho_d z_{d(df)}. \tag{27}$$

We can now substitute Eqs. (26) and (27) into the Clausius-Clapeyron equation, and expand to first order in $1/z_{d(df)}$. Since the variation of $N_{c(df)}$ and $N_{3(cf)}$ is negligible on this scale, we can substitute their values at D. The result is

$$d\mu_4/d\mu_3 = -X_{3d}/X_{4d} - \frac{N^D_{c(df)} - N^D_{3(cf)}}{z_{d(df)}X_{4d}\rho_d}, \tag{28}$$

which can be rewritten [using Eq. (25) for $z_{d(df)}$]

$$X_{3d}d\mu_3 + X_{4d}d\mu_4 = -(-\Delta\mu')^{1/3}/a_D, \tag{29}$$

where we have defined a new combination of parameters $a_D = \rho_d(\Delta C_3^{d\omega})^{1/3}/(n^D_{c(df)} - n^D_{3(cf)})$. Since $\Delta\mu' = -\Delta\omega_d/\rho_d$ and $X_{3d}d\mu_3 + X_{4d}d\mu_4 = -d\omega_d/\rho_d$, the integration is trivial, yielding

$$\frac{3}{2}a_D(-\Delta\mu')^{2/3} = -\Delta\mu_3, \tag{30}$$

a result very similar to Eq. (15), but with an extra minus sign, and where the $\Delta\mu$'s are now measured from D.

The curve expressed by Eq. (30) does not quite pass through the point X determined in Sec. III A 1, and so we adjust it by adding a term of the next leading order,

$$\Delta\mu' = -\left[\left(\frac{-\Delta\mu_3}{1.03}\right)^{3/2} + 1.02\Delta\mu_3^2\right]. \tag{31}$$

B. $T > 0$ film phase diagram for Cs substrates

To determine the $T > 0$ film phase diagram, we extend the lines WX, XY, and XD as sheets ending in critical lines. To this we must add the sheet of Kosterlitz-Thouless transitions in the films. The results are shown in Fig. 4 which displays the film transitions only, for clarity. For the bulk transitions see Fig. 1. Constant temperature cuts through the combined bulk and film phase diagrams at $T = 0.4$, 0.75, 1.0, and 1.5 K are shown in Fig. 5.

1. Wetting curve

The wetting curve WW_0 was determined as in Pettersen and Saam,[9] from the wetting condition $\sigma_4(\mu_3, T) + \sigma_{4w} = \sigma_{wv}$ where $\sigma_4(\mu_3, T)$ is the surface tension of ^{4}He

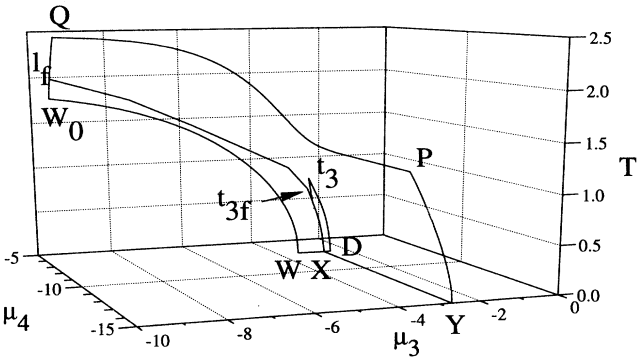

FIG. 4. The phase diagram of ^{3}He-^{4}He mixture films adsorbed on a Cs substrate. The sheet $WXYPQW_0$ is the prewetting sheet with critical line PQ; the sheet XDt_3t_{3f} is the isotopic separation sheet with tricritical line t_3t_{3f}. The curve WW_0 is a line of wetting transitions where the prewetting sheet is tangent to the bulk liquid-vapor coexistence sheet. The curve $l_ft_{3f}t_3$ represents two edges of the λ transition sheet in the film. (Bulk phase transitions are not shown, for the sake of clarity.) μ_3, μ_4, and T are in K.

with ^{3}He impurities at the liquid-vapor interface, and σ_{wv} and σ_{4w} are the surface tensions between cesium and the vapor and liquid, respectively. When the amount of ^{3}He is small, $\sigma_4(\mu_3, T) = \sigma_4^0(T) - \phi(\mu_3)$, where σ_4^0 is the surface tension of pure ^{4}He, and $\phi(\mu_3, T)$ is the spreading pressure of a two-dimensional Fermi gas with binding energy $-(E_s + E_3)$ and effective mass m_{3s}=1.45 m_3.[21] [The equations determining $\phi(\mu_3)$ are given by Edwards *et al.*[37]] The cesium surface tensions appear only as a combination which can be determined from the wetting temperature T_W = 1.95 K (Ref. 6) of pure ^{4}He: $\sigma_{wv} - \sigma_{4w} = \sigma_4^0(T_W)$=0.306 erg/cm^2. Then μ_4 is determined from μ_3 and T using the regular solution models described in Secs. II B 2 and II B 4.

2. *Prewetting critical sheet*

We begin this subsection by considering the critical point of the prewetting transition. For pure ^{3}He and pure ^{4}He, the prewetting transition ends at a critical point [T = 2.5 K (Ref. 6) and $\mu_4 - \mu_4^0 = -0.05$ K for ^{4}He (Ref. 2), while T = 1.3 K and $\mu_3 - \mu_3^0 = -0.23$ K for ^{3}He (Ref. 32)] where the difference in surface number density between the thick and thin phases vanishes. This critical point is analogous to the bulk liquid-gas critical point. Just as for the bulk, then, for intermediate film concentrations we expect a line of critical points interpolating between the two limit points. Lacking a detailed theory of the critical line, we show it in the phase diagram as a scaled copy of the bulk critical line. The line of prewetting critical points, PQ in Fig. 4, is expected to be in the two-dimensional (2D) Ising universality class. The prewetting sheet $WXYPQW_0$ then connects the prewetting critical line PQ and the $T = 0$ prewetting line WXY of Fig. 3. The wetting curve WW_0 is a line of contact where the prewetting sheet touches the bulk coexistence sheet *atbcd* of Fig. 1.

3. *Triple line*

The triple point X between the thin, dilute, and concentrated phases in the film extends to $T > 0$ as the triple line Xt_{3f} of Fig. 4, again analogous to the bulk triple line. Once again we show it in the phase diagram as a scaled copy of the bulk triple line. Two-dimensional critical points typically occur at temperatures 2/3 of the

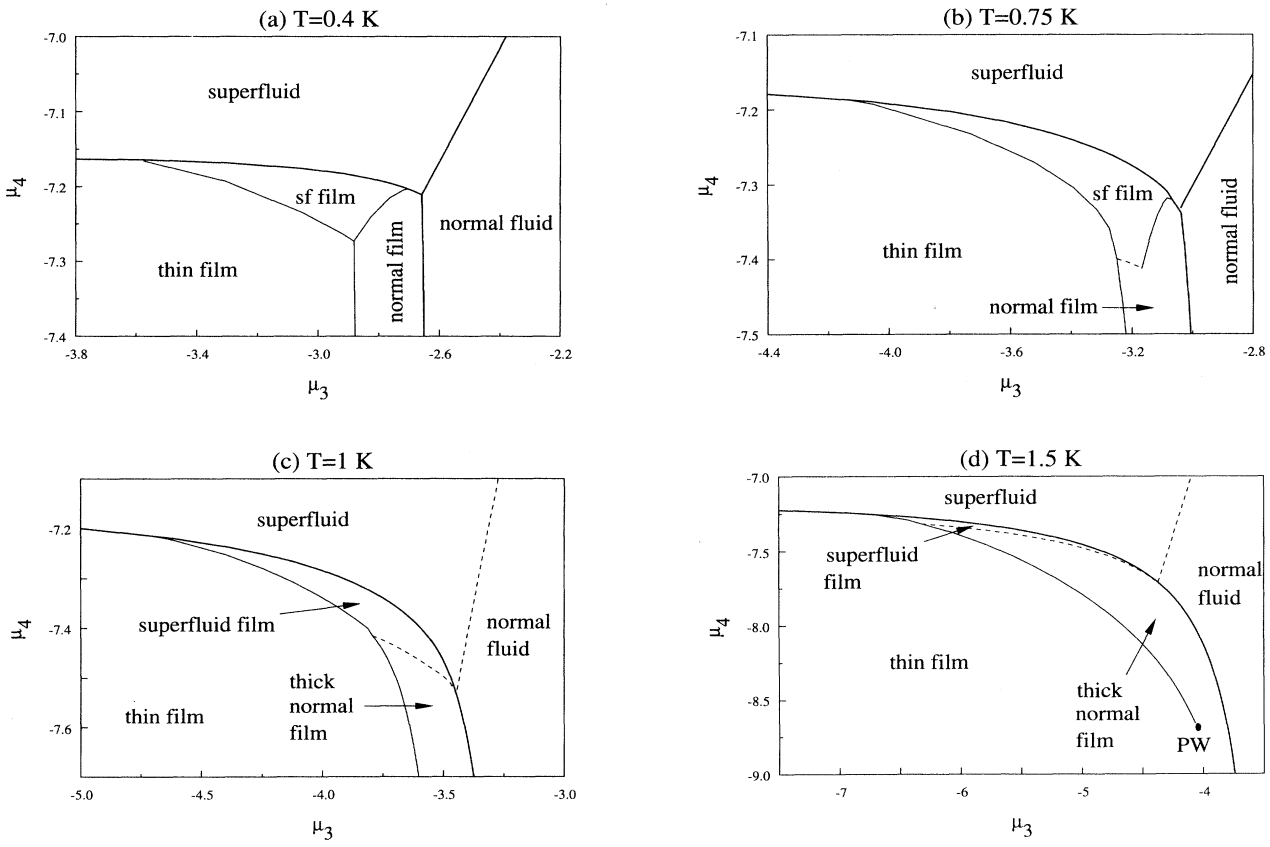

FIG. 5. Constant temperature slices through the combined bulk and film phase diagrams of ^{3}He-^{4}He mixture films adsorbed on Cs. (a) T=0.4 K, (b) T=0.75 K, (c) T=1 K, (d) T=1.5 K. Solid lines represent first-order phase transitions; dashed lines are λ transitions. μ_3 and μ_4 are in K.

bulk value, and so the film triple line probably ends in a tricritical point analogous to the bulk tricritical point at a temperature of about 0.6 K. The film tricritical point then lies well below any likely value of the film critical line, a situation analogous to that which obtains for the bulk tricritical point. In this case the point t_{3f} is a tricritical end point of a type for which critical exponents are, to our knowledge, unknown.

4. Dewetting transition and phase separation sheet

Next, we shall show that the dewetting transition D persists at $T > 0$ and approaches the bulk tricritical point. Following the result expressed in Eq. (21),

$$\sigma_{d3} + (\sigma_{dw} - \sigma_{w3}) = \frac{3}{2}\rho_3 \left[(\Delta C_3^{3w})^{1/3} - (\Delta C_3^{3d})^{1/3}\right] \times(-\Delta\mu_3)^{2/3}. \quad (32)$$

Now as we approach the bulk tricritical point, $\sigma_{d3} \propto (T_3 - T)^2$,[38,39] while $\sigma_{dw} - \sigma_{w3} \propto (T_3 - T)^{\beta_1}$, where the critical exponent β_1 is not known for a tricritical point. For a critical point, β_1=0.8; for a tricritical point in mean field theory, β_1=3/4.[40] Within mean field theory, then, the dewetting transition approaches the bulk tricritical point as $(T_3 - T)^{\beta_1} \propto (-\Delta\mu_3)^{2/3}$, where $\Delta\mu_3$ is measured from the triple line.

The film phase separation curve at 0 K runs from the film triple point X to the dewetting point D. At $T > 0$, the triple point has been traced to the film tricritical point, and the dewetting point D has been traced to the bulk tricritical point. Phase separation in the film thus extends at $T > 0$ to a sheet ending in a line of critical points running from the film tricritical point to the bulk tricritical point. This is analogous to the line of tricritical points for the bulk liquid under pressure (densities higher than at saturated vapor pressure). Interesting 2D to 3D crossover effects would be expected as this line approaches the bulk tricritical point t_3 and its associated critical film becomes infinite in thickness.

5. λ transition and λ sheet

Next we examine the λ transition in the film. In the bulk, the λ transition is a sheet which intersects the liquid-gas coexistence sheet at SVP and terminates on the line of isotopic separation tricritical points. The bulk λ transition lies above the wetting transition in the dilute film, and so clearly the λ transition in the film must approach the bulk λ transition as the film approaches infinite thickness. For pure ^{4}He, it is found empirically that the lambda transition obeys the law[2]

$$\Delta\mu_4 = -\frac{\Delta C_3}{\ell_0^3}\left(\frac{T_\lambda - T_c}{T_\lambda}\right)^{3\hat{\nu}},$$

with $\hat{\nu} = 0.52$ and $\ell_0 = 12.3$ Å. We extend this empirical formula to mixtures by allowing T_λ to depend on concentration, and estimating the concentration dependence of ΔC_3 by $\Delta C_3 = C_3^{4w} - (\rho_d/\rho_4)C_3^{44}$. We use this formula to construct the λ transition curves in the constant T diagrams of Fig. 5. The λ transition sheet must end at the line of phase separation tricritical points $t_{3f}t$, as mentioned above.

6. Discussion of the constant temperature sections

Figure 5 shows a series of constant temperature sections of the combined bulk and film phase diagrams. The slice at 0.4 K shows little change from 0 K, except for the disappearance of the 0 K phase transitions. At 0.75 K, the section is above the film tricritical end point, but below the bulk tricritical point. The section cuts partly through the film isotopic separation sheet and partly through the film λ sheet. At 1 K, the section is above both film and bulk tricritical points, and the λ transition completely takes the place of phase separation. The section at 1.5 K is above the critical point for prewetting in ^{3}He; a prewetting critical point appears where the section cuts the prewetting critical line.

C. Other possibilities for Cs substrates

The recent experiments of Rutledge and Taborek[41] indicate that the critical point for prewetting in pure ^{3}He may be at a temperature substantially below 1.26 K. Here we consider the possibility that ^{3}He wets Cs without a prewetting transition even at $T = 0$.

At $T = 0$, along the line XY in Fig. 3, the film phase is pure ^{3}He, and so if prewetting is absent for pure ^{3}He, the entire line XY is absent. The arguments concerning the wetting transition at the point W and the dewetting transition at D are unaffected, however. Thus the zero-temperature phase diagram must be as shown in Fig. 6. The prewetting transition is the curve WD separating

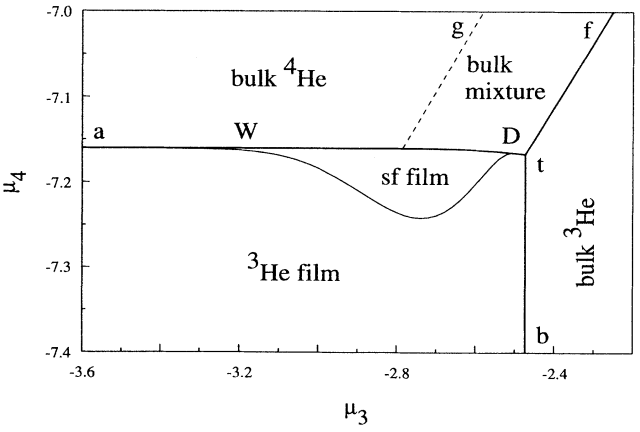

FIG. 6. The $T = 0$ phase diagram of ^{3}He-^{4}He mixture films adsorbed on a Cs substrate under the hypothesis that ^{3}He does not have a prewetting transition. Curve WD is a prewetting transition. μ_3 and μ_4 are in K.

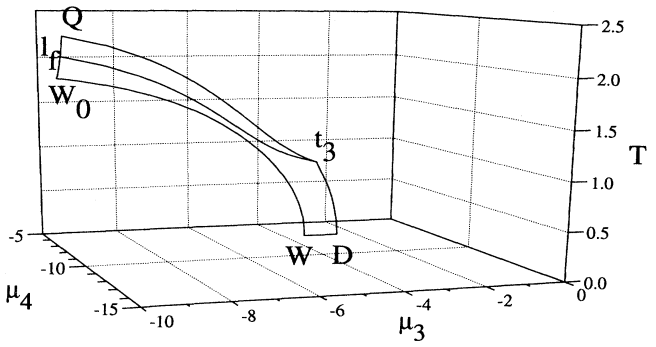

FIG. 7. The phase diagram of ^{3}He-^{4}He mixture films adsorbed on a Cs substrate under the hypothesis that ^{3}He does not have a prewetting transition. WDt_3QW_0 is the prewetting sheet with critical line Qt_3; l_ft_3 represents an edge of the λ transition sheet. μ_3, μ_4, and T are in K.

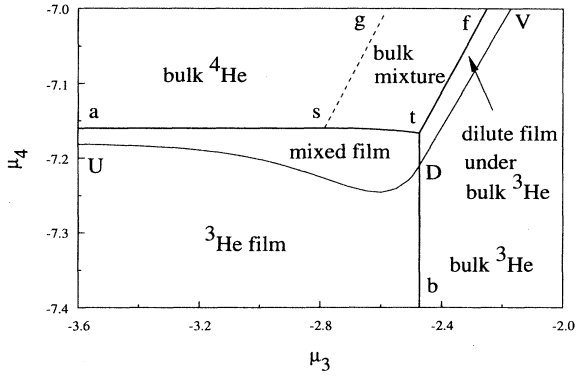

FIG. 8. Sketch of the phase diagram of ^{3}He-^{4}He mixture films adsorbed on Na at $T = 0$. The bulk features are reproduced from Fig. 2. The curve UDV is a prewetting transition for the film: Along segment UD it is a prewetting transition for a ^{4}He film under a ^{3}He film; along DV it is a prewetting transition for a ^{4}He film under bulk concentrated ^{3}He. The region labeled "^{3}He film" is bounded on the left by a vertical line of $T = 0$ phase transitions (not shown) at $\mu_3 = -\epsilon_{3B}$, where the binding energy ϵ_{3B} of ^{3}He atoms on Na is approximately 5 K. μ_3 and μ_4 are in K.

the superfluid film from the ^{3}He film in the phase diagram.

Extending the prewetting curve WD to $T > 0$ as before produces a prewetting sheet ending in a prewetting critical line, sketched as Qt_3 in Fig. 7. The edges WW_0 and Dt_3 of the prewetting sheet are unchanged, the same as in Fig. 4. The prewetting critical line must approach the bulk tricritical point t_3. For the prewetting transition is also an isotopic separation transition, and since the film phases near t_3 are very thick, the critical line for isotopic separation in the film must approach the bulk isotopic separation tricritical line. A similar argument holds for the λ line l_ft_3 where the λ sheet meets the prewetting sheet.

In Fig. 7, we have shown the λ line l_ft_3 and the prewetting critical line Qt_3 approaching t_3 tangentially to one another, which seems the most likely possibility. It is also possible for the two curves to coincide for some distance, forming a tricritical line analogous to the isotopic separation tricritical lines t_3ft_3 of Fig. 4 or t_3e of Fig. 1.

IV. CONSTRUCTION OF THE FILM PHASE DIAGRAMS FOR OTHER ALKALI-METAL SUBSTRATES

A. Sodium substrates at 0 K

Sodium is a slightly stronger binding substrate than cesium. It has been predicted that at 0 K, ^{4}He wets sodium with a prewetting transition (compare nonwetting of ^{4}He on Cs),[1] and ^{3}He wets sodium completely, with no prewetting transition.[32] Figure 8 shows the $T = 0$ phase diagram for mixture films on sodium.

To trace the ^{4}He prewetting transition into mixed films, we again compare the free energies of the dilute and concentrated films at the triple point t, as in Sec. III A 3.

The liquid-substrate surface tensions to a good approximation are[1] given for $i = 3, d$ by $\sigma_{wi} = \sigma_{wv} + \sigma_{iv} - 0.6\rho_i(C_3D^2)^{1/3}$, where $\sigma_{wv} + \sigma_{iv}$ is the energy cost of introducing surfaces in the substrate and the liquid, and the last term is the potential energy of the two media in contact, in the so-called "simple model" of the substrate van der Waals potential

$$V(z) = \frac{4C_3^3}{27D^2z^9} - \frac{C_3}{z^3},$$

with parameters C_3 and D. Then we have

$$\begin{aligned}\omega_{df} - \omega_{cf} &= (\sigma_{dw} + \sigma_{d3} + \sigma_{3v}) - (\sigma_{3w} + \sigma_{3v}) \\ &\approx (\sigma_{dv} + \sigma_{d3} - \sigma_{3v}) + 0.6(\rho_3 - \rho_d)(C_3D^2)^{1/3}.\end{aligned} \tag{33}$$

Saam *et al.*[2] give values $C_3 = 1070$ K Å^3 and D=10.4 K for helium adsorbed on sodium, but they argue that the observed value of the wetting transition temperature for pure ^{4}He on Cs indicates that this underestimates the value of D by about 4 K, and so we take D=14.4 K. The surface tension σ_{dv} cannot be measured, since a layer of ^{3}He spontaneously forms at the free dilute liquid surface. We shall take $\sigma_{dv} \approx \sigma_{4v}$, which is certainly an overestimate.

Using these values, at the triple point, we find

$$\omega_{df} - \omega_{cf} \leq -0.023 \text{ K Å}^{-2}. \tag{34}$$

The negative value for this combination of surface tensions implies that the dilute phase is the stable phase of the film at the point t, and therefore that the point D lies on the curve tb. In this case D is not a dewetting

transition. We note that that this result is equivalent to

$$\omega_{df} - \omega_{cf} = \sigma_{dw} + \sigma_{d3} - \sigma_{3w} < 0, \tag{35}$$

which implies that a layer of the phase dilute in ^{3}He does form at the interface between ^{3}He and sodium, which is confirmed by an unpublished calculation of Saam and Treiner.[34] (Had we taken D=10.4 K, our result would have had the opposite sign; this is the case for rubidium and potassium substrates, which we shall discuss below. Sodium is therefore a marginal case.)

As one increases μ_3 along the liquid-gas phase boundary there is a jump at D from a wetting film of ^{3}He below D to a wetting film of ^{3}He with a thin layer of dilute phase film interposed between it and the sodium substrate. The line DV is thus a prewetting (thin-thick) transition for a ^{4}He layer forming under the ^{3}He film. As one moves along the prewetting line UDV from the vapor region across the bulk liquid-vapor coexistence line to the pure liquid ^{3}He phase, the prewetting transition of the dilute film becomes a condensation of a ^{4}He rich film under bulk ^{3}He. The presence of such a film is typical of strong-binding substrates and has been studied, for example, on chromium substrates by Romagnan *et al.*[42] and Nakamura *et al.*[43] on Ta substrates.

Note that the region in Fig. 8 labeled ^{3}He film is bounded on the left by a vertical line of $T = 0$ phase transitions (not shown) at $\mu_3 = -\epsilon_{3B}$, where the binding energy ϵ_{3B} of ^{3}He atoms on Na is approximately 5 K.

The location of the point D is determined by making a model of the surface free energy excess for the dilute film for finite thicknesses:[44]

$$\omega_{df} = \sigma_{\omega d} + \sigma_{d3} + \sigma_{3v} + \frac{(\rho_d - \rho_3)\Delta C_3^{d\omega}}{z_{d(df)}^2} - \rho_d z_{d(df)} \Delta\mu', \tag{36}$$

where minimizing with respect to $z_{d(df)}$ yields

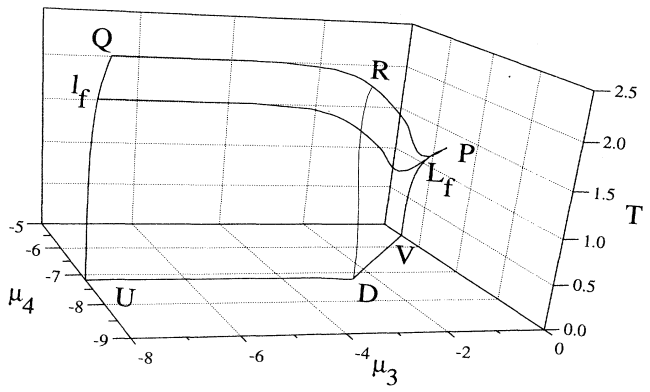

FIG. 9. Sketch of the phase diagram of ^{3}He-^{4}He mixture films adsorbed on Na. $UVPQ$ is the prewetting sheet for the dilute film; $l_f L_f$ is the edge of the λ transition sheet for the film, where it meets the prewetting sheet. The curve DR shows the intersection of the prewetting sheet $UVPQ$ with the bulk liquid-vapor coexistence sheet. μ_3, μ_4, and T are in K.

$$z_{d(df)} = \left(\frac{-(\rho_d - \rho_3)\Delta C_3^{dw}}{\rho_d \Delta\mu'}\right)^{1/3}. \tag{37}$$

The result is that, at D,

$$\frac{3}{2}\rho_d^{2/3}(\rho_d - \rho_3)^{1/3}(\Delta C_3^{dw})^{1/3}(-\Delta\mu')^{2/3} = -(\sigma_{4w} + \sigma_{d3} - \sigma_{3w}),$$

whence $\Delta\mu' = -0.042$ K, and the ^{4}He underlayer at point D is 17 Å thick.

The slope of the curve UDV at D cannot be found without a knowledge of corrections to the asymptotic van der Waals form of the potential. The slope in Fig. 8 is a sketch.

B. Sodium substrates at $T > 0$

Several possibilities exist for the phase diagram for sodium at $T > 0$. One possibility, sketched in Fig. 9, is that as was the case for cesium substrates, the prewetting transition will extend to higher temperatures as a prewetting sheet ending in a prewetting critical line. The bulk λ transition sheet will extend into the dilute film region as a Kosterlitz-Thouless transition in the ^{4}He underlayer. The λ transition will also extend from the bulk tricritical line as a Kosterlitz-Thouless transition in the dilute film adsorbed under bulk ^{3}He. The existence of a normal film at the wall under bulk ^{3}He, and the critical point associated with the thin-thick transition in this layer, has not to our knowledge been experimentally demonstrated, though the observations of Romagnan *et al.*[42] for the case of a chromium substrate are consistent with this picture. The observations of Nakamura *et al.*[43] on a Ta substrate, which show a continuous formation of a ^{4}He film under bulk ^{3}He, are consistent with an experimental trajectory passing behind the section $RDVP$ of the prewetting sheet of Fig. 9, without intersecting it, and approaching the triple line with decreasing temperature.

C. Rb and K

Rubidium and potassium substrates fall into a class of behavior intermediate between cesium and sodium. Pricaupenko and Treiner[32] predict that ^{3}He wets both Cs and K at $T = 0$ with a prewetting transition, and so we may presume that the same is true for Rb, which falls between Cs and K in the periodic table. This differs from the case of Na, which is strongly enough binding that ^{3}He wets at $T = 0$ without a prewetting transition.

On the other hand, ^{4}He exhibits $T = 0$ prewetting on Na, and so it may be expected to show prewetting or possibly even nonwetting on Rb and K at $T = 0$. If the value of the parameter D is corrected by the same 4 K that we used in Sec. IV A, then the "simple model" predicts that both Rb and K, unlike Cs, are wetted by ^{4}He at 0 K, though the case of Rb is marginal. Experiments of Nacher *et al.*[45] indicate ^{4}He wets Rb to low temperatures, but Wyatt *et al.*[46] have presented evidence ^{4}He

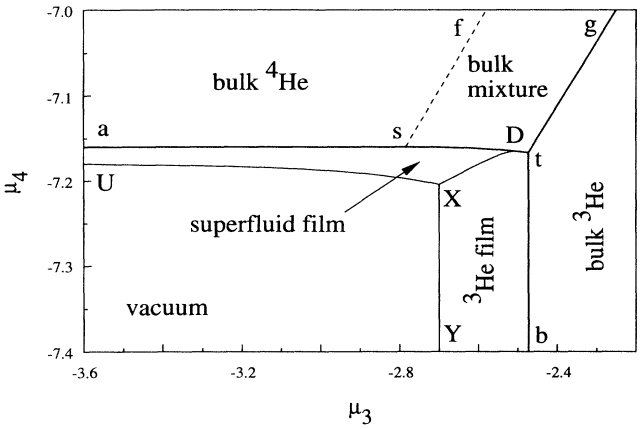

FIG. 10. Sketch of the phase diagram of ^{3}He-^{4}He mixture films adsorbed on Rb or K at $T = 0$ showing the same features as the Cs phase diagram (Fig. 3) except for the wetting transition W, which has moved off to minus infinity to be replaced by prewetting at the point U. μ_3 and μ_4 are in K.

does not wet Rb below 309 mK.

To find the location of the point D, we use the "simple model" with values from Ref. 1 (C_3= 754 K Å^3, D=9 K adjusted for Rb; C_3= 812 K Å^3, D=10.3 K adjusted for K) to find the value of the combination of surface tensions

$$\omega_{df} - \omega_{cf} = \sigma_{dw} + \sigma_{34} - \sigma_{3w} = \begin{cases} +0.041 \text{ K (Rb)} \\ +0.026 \text{ K (K)}. \end{cases} \quad (38)$$

Thus, as is the case for Cs, a ^{4}He film will not wet either Rb or K walls under bulk concentrated ^{3}He, and the point D of Fig. 3 for these cases lies on the curve at, to the left of the triple point t.

To conclude, the phase diagrams for Rb and K, sketched in Fig. 10, are similar to that for Cs, except that in both cases the intersection of the prewetting sheet and the bulk dilute liquid-vapor coexistence sheet and the line of contact WW_0 are absent. If ^{4}He is ultimately shown not to wet Rb at T=0, then Rb will have the same type of phase diagram as Cs (Fig. 3).

V. DISCUSSION AND CONCLUSIONS

The phase diagram for ^{3}He-^{4}He mixture films on Cs substrates has been quantitatively derived from a minimum of information: the experimentally measured wetting temperature and location of the prewetting critical point in $\mu_4 - T$ for pure ^{4}He on Cs, and the theoretically predicted prewetting chemical potential and prewetting critical temperature for pure ^{3}He, in addition to the knowledge of the properties of bulk mixtures. Similar phase diagrams have been sketched for films adsorbed on Rb, K, and Na substrates.

It is not practical to display these phase diagrams in terms of variables such as the concentration of the film (surface excess concentration) and relative saturation, p/p_0, where p is the pressure and p_0 is the saturated vapor pressure. Because p_0 depends on the concentration of the film or liquid chosen for reference, regions corresponding to different phases overlap on such a diagram. In the film part of the phase diagram, at temperatures sufficiently below the critical line, the chemical potentials can be converted to partial pressures of each isotope, using the Sackur-Tetrode equation for the ideal gas,

$$p_i = (k_B T)^{5/2} \left(\frac{m_i}{2\pi\hbar^2}\right)^{3/2} e^{\mu_i/k_B T},$$

with p_i, m_i, and μ_i the partial pressure, isotopic mass, and chemical potential of the ith isotope ($i = 3, 4$).

It is difficult, in any case, to control the film concentration experimentally, except in cases of macroscopically thick films or very low temperatures: Since the concentrations of film and vapor are not equal, an exchange of isotopes will take place between these two reservoirs as external parameters such as temperature are changed. The chemical potentials can be directly controlled by having the substrate open to a reservoir of liquid or vapor, sufficiently large so as not to be depleted by the condensation of the film.

The phase diagram for ^{3}He-^{4}He mixtures on Cs shows several novel features. Along the curve WW_0, ^{3}He acts as a surfactant, lowering the wetting transition temperature from the value 1.95 K for pure ^{4}He to zero at the point W. At 0 K, along the curve WD, ^{3}He induces wetting of the mixed film, until at the point D, a pure ^{3}He film displaces the mixed film. The solubility of ^{3}He in ^{4}He on Cs substrates is thus lowered to 5.2%. The point D is an example of triple-point-induced dewetting, which was predicted some time ago,[35] but has not yet been conclusively demonstrated. The ^{3}He-^{4}He/Cs system may prove particularly amenable to the observation of this effect. Note also that the location of W_0 may be varied by the use of cesium-plated quartz substrates.[7]

As the temperature is raised, the dewetting transition approaches the bulk tricritical point t_3, as shown in Sec. III B 4. The approach is governed by the critical exponent β_1, which governs the difference in surface tensions $\sigma_{4w} - \sigma_{3w}$. For a tricritical point, β_1 is not known even theoretically. It should be possible to measure β_1 in the ^{3}He-^{4}He/Cs system.

The isotopic separation for the film exhibits a tricritical point which undergoes crossover from three-dimensional to two-dimensional behavior along the curve $t_3 t_{3f}$ of Fig. 4. Crossover exponents would be of interest to measure.

The interface between bulk concentrated ^{3}He and Cs, Rb, and K is not wetted by a film of the dilute phase. Third-sound experiments or capacitative measurements of dielectric variations[42] would test this prediction. Most substrates are wetted by a superfluid film under bulk concentrated ^{3}He. This film acts as a nucleus for the isotopic separation of supersaturated solutions. The absence of such a film raises the possibility of forming supersaturated solutions of ^{4}He in ^{3}He in vessels with Cs-, Rb-, or K-coated walls. It would be interesting to search for

Bose condensation of the ^{4}He in a supersaturated solution. Bose condensation can only occur if the interaction between ^{4}He quasiparticles in solution is repulsive. The sign of this interaction is not known, though there is a suggestion that it may be positive.[47] Superfluidity of dissolved ^{4}He may have been observed in aerogel.[48]

The dilute phase does wet the interface between bulk concentrated ^{3}He and Na walls, which is the situation for ordinary substrates. We have speculated that the prewetting transition for this film has a critical point above the λ transition. Although the superfluid transition[42] has been observed, the thin-thick (prewetting) transition to a superfluid film in dilute films under ^{3}He and the existence of a critical point would be new phenomenona. Measurements with narrow-gap capacitors, such as those of Nakamura and co-workers,[43] would be able to demonstrate the existence of a critical point in the thin-thick transition.

While great progress has been made in the experimental verification of theories of wetting in the helium-alkali systems, the richness of the system has not yet been exhausted. Mixture films provide a system in which the parameters of the theory may be adjusted continuously by varying the isotopic concentration. Many new phenomena remain to be discovered and explored.

ACKNOWLEDGMENTS

We thank Jacques Treiner for discussions near the inception of this work. This research has been supported in part by National Science Foundation Grant No. DMR-9014679.

[1] E. Cheng, M. W. Cole, W. F. Saam, and J. Treiner, Phys. Rev. Lett. **67**, 1007 (1991); Phys. Rev. B **46**, 13967 (1992); **47**, 14661(E) (1993); E. Cheng, M. W. Cole, J. Dupont-Roc, W. F. Saam, and J. Treiner, Rev. Mod. Phys. **65**, 557 (1993).

[2] W. F. Saam, J. Treiner, E. Cheng, and M. W. Cole, J. Low Temp. Phys. **89**, 637 (1992).

[3] P. J. Nacher and J. Dupont-Roc, Phys. Rev. Lett. **67**, 2966 (1991); N. Bigelow, P. J. Nacher, and J. Dupont-Roc, J. Low Temp. Phys. **89**, 135 (1992).

[4] K. S. Ketola, S. Wang, and R. B. Hallock, Phys. Rev. Lett. **68**, 201 (1992); S. K. Mukherjee, D. P. Druist, and M. H. W. Chan, J. Low Temp. Phys. **87**, 113 (1992).

[5] P. Taborek and J. E. Rutledge, Phys. Rev. Lett. **68**, 2184 (1992).

[6] J. E. Rutledge and P. Taborek, Phys. Rev. Lett. **69**, 937 (1992).

[7] P. Taborek and J. E. Rutledge, Phys. Rev. Lett. **71**, 263 (1993).

[8] E. Cheng, G. Mistura, H. C. Lee, M. H. W. Chan, M. W. Cole, C. Carraro, W. Saam, and F. Toigo, Phys. Rev. Lett. **70**, 1854 (1993).

[9] M. S. Pettersen and W. F. Saam, J. Low Temp. Phys. **90**, 159 (1993).

[10] K. S. Ketola and R. B. Hallock, Phys. Rev. Lett. **71**, 3295 (1993).

[11] W. Hsu, D. Pines, and C. H. Aldrich, Phys. Rev. B **33**, 6057 (1986); **32**, 7179 (1985).

[12] P. Seligman, D. O. Edwards, R. E. Sarwinski, and J. T. Tough, Phys. Rev. **181**, 415 (1969).

[13] C. Ebner and D. O. Edwards, Phys. Rep. **2**, 77 (1970).

[14] R. M. Bowley, J. Low Temp. Phys. **61**, 291 (1975); **71**, 319 (1988).

[15] R. Radebaugh, *Thermodynamic properties of ^{3}He-^{4}He Solutions with Applications to the ^{3}He-^{4}He Dilution Refrigerator*, NBS Technical Note 362 (U. S. Department of Commerce, Washington, D.C., 1967).

[16] J. G. M. Kuerten, C. A. M. Castelijns, A. T. A. M. de Waele, and H. M. Gijsman, Cryogenics **25**, 419 (1985).

[17] W. P. Halperin and E. Varoquaux, in *Helium 3*, edited by Halperin and Pitaevskii (North-Holland, Amsterdam, 1990), p. 510.

[18] J. Bardeen, G. Baym, and D. Pines, Phys. Rev. **156**, 207 (1967).

[19] A. E. Watson, J. D. Reppy, and R. C. Richardson, Phys. Rev. **188**, 384 (1969).

[20] A. F. Andreev, Zh. Eksp. Teor. Fiz. **50**, 1415 (1965) [Sov. Phys. JETP **23**, 939 (1966)]; K. N. Zinov'eva and S. T. Bolarev, *ibid.* **29**, 585 (1969) [*ibid.* **56**, 1089 (1969)].

[21] See, e.g., D. O. Edwards and W. F. Saam, in *Progress in Low Temperature Physics*, edited by D. F. Brewer (North-Holland, New York, 1978), Vol. VIIa, Chap. 4.

[22] S. S. Leung and R. B. Griffiths, Phys. Rev. A **8**, 2670, 1973.

[23] V. V. Sychev, A. A. Vasserman, A. D. Kozlov, G. A. Spiridonov, and V. A. Tsymarny, in *Thermodynamic Properties of Helium*, edited by T. B. Selover (Hemisphere, Berlin, 1987).

[24] B. Wallace and H. Meyer, Phys. Rev. A **2**, 1563 (1970).

[25] Computer code PSIPLOT, version 3, Poly Software International, Salt Lake City, 1994.

[26] R. de Bruyn Ouboter, J. J. M. Beenakker, and K. W. Taconis, Physica **25**, 1162 (1959).

[27] L. M. J. Van de Klundert, M. R. E. Bos, J. A. M. van der Meij, and H. J. Steffens, Phys. Lett. **62A**, 487 (1977).

[28] J. del Cueto, R. L. Johnson, T. Rohde, F. H. Wirth, and E. H. Graf, J. Phys. (Paris) Colloq. **41**, C7-133 (1980).

[29] J. P. Laheurte, J. Low Temp. Phys. **12**, 127 (1973).

[30] J. Wilks, *Properties of Liquid and Solid Helium* (Clarendon Press, Oxford, 1967).

[31] S. G. Sydoriak and T. R. Roberts, Phys. Rev. **118**, 901 (1960).

[32] L. Pricaupenko and J. Treiner, Phys. Rev. Lett. **72**, 2215 (1994).

[33] See, e.g., C. Ebner, W. F. Saam, and A. K. Sen, Phys. Rev. B **32**, 1558 (1985).

[34] W. F. Saam and J. Treiner (unpublished).

[35] R. Pandit and M. E. Fisher, Phys. Rev. Lett. **51**, 1772 (1983); see also C. Ebner, Phys. Rev. B **28**, 2890 (1983).

[36] See, e.g., S. Dietrich, in *Phase Transitions and Critical Phenomena*, edited by C. Domb and J. Lebowitz (Academic, New York, 1988), Vol. 12.

[37] D. O. Edwards, S. Y. Shen, J. R. Eckardt, P. P. Fatouros,

and F. M. Gasparini, Phys. Rev. B **12**, 892 (1975).
[38] M. Papoular, Phys. Fluids **17**, 1038 (1974).
[39] P. Leiderer, H. Poisel, and M. Wanner, J. Low Temp. Phys. **28**, 167 (1977).
[40] K. Binder, in *Phase Transitions and Critical Phenomena*, edited by C. Domb and M. S. Green (Academic, London, 1983), Vol. 8.
[41] J. E. Rutledge and P. Taborek, J. Low Temp. Phys. **95**, 405 (1994).
[42] J.-P. Romagnan, J.-P. Laheurte, J.-C. Noiray, and W. F. Saam, J. Low Temp. Phys. **30**, 425 (1978), and references therein.
[43] M. Nakamura, Y. Fujii, T. Shigi, and K. Nagao, J. Phys. Soc. Jpn. **57**, 1676 (1988); M. Nakamura, G. Shirota, T. Shigematsu, K. Nagao, Y. Fujii, M. Namaguchi, and T. Shigi, Physica **B165&166**, 517 (1990).
[44] M. S. Pettersen, M. J. Lysek, and D. L. Goodstein, Phys. Rev. B **40**, 4938 (1989).
[45] P. J. Nacher, B. Demolder, and J. Dupont-Roc, Physica B **194-196**, 975 (1994); B. Demolder, N. Bigelow, P. J. Nacher, and J. Dupont-Roc, J. Low Temp. Phys. **98**, 91 (1995).
[46] A. F. G. Wyatt, J. Klier, and P. Stefanyi, Phys. Rev. Lett. **74**, 1151 (1995).
[47] D. O. Edwards, M. S. Pettersen, and T. G. Culman, J. Low Temp. Phys. **89**, 831 (1992).
[48] J. Ma, S. B. Kim, L. W. Hrubesh, and M. H. W. Chan, J. Low Temp. Phys. **93**, 945 (1993).